Neuropharmacology 56 (2009) 30–36

Contents lists available at ScienceDirect

Neuropharmacology

journal homepage: www.elsevier.com/locate/neuropharm

The excitatory postsynaptic density is a size exclusion diffusion environment

Marianne L. Renner [a,1], Laurent Cognet [b], Brahim Lounis [b], Antoine Triller [c], Daniel Choquet [a,*]

[a] Physiologie Cellulaire de la Synapse, CNRS (UMR 5091), Université Bordeaux, Institut François Magendie, 146 rue Leo Saignat, 33077 Bordeaux Cedex, France
[b] Centre de Physique Moléculaire Optique et Hertzienne, CNRS (UMR 5798), Université Bordeaux, 351 Cours de la Libération, 33405 Talence Cedex, France
[c] Biologie Cellulaire de la Synapse, INSERM U 789, Ecole Normale Supérieure, 75005 Paris, France

ARTICLE INFO

Article history:
Received 29 April 2008
Received in revised form 3 July 2008
Accepted 8 July 2008

Keywords:
Single molecule tracking
AMPA receptors
Lipids
Postsynaptic density
Synaptic transmission
Brownian diffusion

ABSTRACT

Receptors are concentrated in the postsynaptic membrane but can enter and exit synapses rapidly during both basal turnover and processes of synaptic plasticity. How the exchange of receptors by lateral diffusion between synaptic and extrasynaptic areas is regulated remains largely unknown. We investigated the structural properties of the postsynaptic membrane that allow these movements by addressing the diffusion behaviors of AMPA receptors (AMPARs) and different lipids. Using single molecule tracking we found that not only AMPARs but also lipids, which are not synaptically enriched, display confined diffusion at synapses. Each molecule type displays a different average confinement area, smaller molecules being confined to smaller areas. Glutamate application increases the mobility of all molecules. The structure of the synaptic membrane is thus probably organized as a size exclusion matrix and this controls the rate of exchange of molecules with the extrasynaptic membrane.

1. Introduction

Memory and learning are thought to be mediated by the dynamic regulation of the efficacy of synaptic transmission. Excitatory neurotransmission is mediated in large part by activation of the postsynaptic AMPAR subtype of glutamate receptors. In recent years, evidence has accumulated that composition of the postsynaptic membrane in AMPA receptors (AMPARs) fluctuates rapidly and that this dynamic accounts for the construction and plasticity of excitatory synapses (Bredt and Nicoll, 2003; Malinow and Malenka, 2002; Sheng and Kim, 2002; Shepherd and Huganir, 2007). However, how receptors can enter and leave synapses still remains unclear.

The mechanisms that underlie changes in the number of functional AMPARs at synapses are thought to include exocytosis and endocytosis from or to intracellular pools as well as exchange between synaptic and extrasynaptic areas by lateral diffusion in the plasma membrane (Choquet and Triller, 2003). For instance, sites of endocytosis are located at a distance from synapses (Blanpied et al., 2002; Racz et al., 2004), suggesting that for basal turnover or during depression of synaptic transmission, receptors have to diffuse out of the synapse before being endocytosed. We and others have demonstrated by single particle and single molecule tracking (SMT) that AMPAR, as well as other types of receptors like GlyR, mGluR5 and NMDAR, diffuse in the neuronal membrane (Borgdorff and Choquet, 2002; Dahan et al., 2003; Groc et al., 2004; Meier et al., 2001; Serge et al., 2002; Tardin et al., 2003). Diffusion of AMPARs not only plays a role in regulating receptor numbers at synapses (Triller and Choquet, 2005), but also participates in the control of fast synaptic transmission by allowing fast replacement of desensitized receptors by naïve ones in milliseconds within the glutamate release zone (Heine et al., 2008). AMPARs display a restricted diffusion behavior which is amplified during maturation, in parallel with synaptogenesis, but still diffuse in mature neurons (Borgdorff and Choquet, 2002; Choquet and Triller, 2003). Moreover, the regulation of receptor diffusion could be involved in synaptic plasticity as it is differentially modulated by protocols that mimic neuronal activity (Groc et al., 2004).

Receptors are concentrated and stabilized at PSDs through interactions with subsynaptic scaffold proteins (Scannevin and Huganir, 2000). For AMPARs, these proteins include PDZ-domain-containing proteins (PSD-95, SAP-97, GRIP, PICK) (Dong et al., 1997; Lisman and Zhabotinsky, 2001; Schnell et al., 2002; Terashima et al., 2004) and TARPs (Chen et al., 2000; Fukata et al., 2005). At PSDs, receptors and their associated proteins show a precise organization. This organization must be reconciled with the ability of receptors to rapidly enter and leave synapses. Strikingly, both immobile and mobile receptors are found inside synapses (Tardin et al., 2003), but mobile synaptic receptors are not free to leave the synapse, their diffusion being confined by unknown mechanisms.

* Corresponding author. Fax: +33 5 57 57 40 82.
E-mail address: dchoquet@u-bordeaux2.fr (D. Choquet).
[1] Present address: Biologie Cellulaire de la Synapse, INSERM U 789, Ecole Normale Supérieure, 75005 Paris, France.

0028-3908/$ – see front matter © 2008 Elsevier Ltd. All rights reserved.
doi:10.1016/j.neuropharm.2008.07.022

In order to investigate the properties of the diffusion environment at the synapse, we followed by SMT the diffusion of AMPARs and that of the membrane lipid DOPE and cholera toxin (ChTx) which binds to ganglioside G_{M1}. This technique not only provides the high resolution needed to study localization of molecules in sub-micrometer membrane domains like the synapse, but also reveals the heterogeneity in diffusion characteristics of the population of molecules by removing the averaging effect of ensemble measurements. Our results show that mobile AMPARs and lipids are confined at mature synapses, albeit to different degrees. Glutamate increases the concentration of mobile receptors allowing them to leave the postsynaptic density by lateral diffusion.

2. Results

2.1. AMPARs, ChTx and DOPE are differentially distributed inside and outside synapses

We used single molecule fluorescence microscopy to localize and to track the movements of either GluA2-subunit-containing AMPARs or two lipids (G_{M1} and DOPE) in 21–27 DIV cultured hippocampal neurons. Ganglioside G_{M1}, a lipid occurring at the outer leaflet of the membrane, is known to form segregated domains in model membranes and is used as a lipid-raft marker (Dietrich et al., 2002; Samsonov et al., 2001). DOPE was chosen as a non-raft lipid probe. We also performed control experiments with $DiIC_{18}$, an artificial fluorescent lipid probe (Spink et al., 1990).

AMPARs and G_{M1} were detected using ligands coupled to a Cy5 dye (respectively, anti-GluA2 antibodies as in Tardin et al. (2003) and cholera toxin (ChTx)) whereas DOPE was directly coupled to a Cy5 dye (Fig. 1A). At the end of our experiments only ~20–25% of AMPARs (Tardin et al., 2003) and ~15–20% of ChTx (not shown) were internalized, so even if internalized fluorophores cannot be distinguished from surface ones the vast majority of the detected molecules were on the surface of neurites.

In order to identify the synaptic molecules we used rhodamine123 (Rh123) to stain synapses (Tardin et al., 2003) (Fig. 1B). AMPARs were found at a 7-fold higher density in areas of synaptic staining ($p < 0.001$, t test) while both lipids studied here displayed a similar relative density inside and outside synapses (Fig. 1C). On average, the detected AMPAR surface density was distributed homogeneously from the centroid of the synaptic staining up to a distance of 0.3 μm away (Fig. 1D) and decreased between 0.3 and 0.6 μm distance to reach the value of the extrasynaptic density. AMPAR enrichment on Rh123 stains indicates that they do indeed correspond to synaptic sites.

Trajectories of individual molecules were reconstructed from sequential images acquired at 18 Hz (Fig. 1A and B). Fig. 1B displays sample DIC images of recording fields overlaid with the synaptic staining and the detected trajectories. Molecules moved over areas of various sizes, ranging from nearly immobile to highly mobile spreading over several μm during our observations (up to 5 s).

2.2. Mobility is reduced in synapses versus non-synaptic areas for all the molecules studied

For each trajectory we calculated the mean square displacement (MSD) as a function of time. We first studied the mobility of molecules using the instantaneous diffusion coefficient D deduced from the initial slope of the MSD function versus time. Within the resolution of our experimental set-up, molecules with D below 0.005 $\mu m^2/s$ could not be distinguished from immobile molecules. For all molecule types, a large mobile fraction was found inside and outside synapses ($53 \pm 3\%$, $58 \pm 2\%$ and $42 \pm 2\%$ for AMPAR, ChTx and DOPE, respectively in extrasynaptic regions and $60 \pm 5\%$, $67 \pm 5\%$, and $42 \pm 3\%$, respectively within synapses) (Fig. 1E). We insured that diffusion of synaptic molecules was not due to the movement of the synaptic stains, which diffused with a D value below our immobility threshold (not shown).

The instantaneous diffusion of mobile molecules is moderately but significantly reduced in synapses. Indeed, on average and for each molecule type, mobile molecules diffused 1.5–2 times less in synaptic than in extrasynaptic areas ($p < 0.001$, Table 1). Comparing the different types of molecules, the mean D values of AMPAR, ChTx and DOPE were at the same order of magnitude in synaptic and extrasynaptic areas (Table 1). However, distributions of D were broad, spanning several orders of magnitude, which suggests the existence of different sub-populations of mobile molecules (Fig. 1E). We did not pursue classification into sub-populations in this context, as more suitable analytical techniques were employed later.

2.3. AMPARs, ChTx and DOPE explore confinement domains of various sizes in synapses

The comparison of D provides no information on the modes of diffusion. In particular, molecules undergoing rapid Brownian diffusion on short time scales can nevertheless be confined in membrane sub-domains. The dependence of the MSD on time is commonly used to extract this information as well as the size of the domain through which the molecule diffuses. For instance, confined diffusion causes the MSD to reach a plateau over time (Saxton and Jacobson, 1997).

Trajectory lengths of individual molecules are limited in time because of the rapid photobleaching of individual dyes. MSD values for individual molecules display high variability, which renders characterization of the types of movement difficult on individual trajectories. We therefore chose a statistical approach to analyze the mean diffusion behavior of sub-populations (Tardin et al., 2003; Schütz et al., 1997). Probability distributions are analyzed on the square displacements r^2 at a given time interval t, pooling together all the trajectories of a given type of molecule (see Section 4). Using this method, two categories of mobile molecules were found at all values of t characterized by a mean square displacement $\langle r^2(\tau)\rangle$ (Fig. 2A). These categories are termed "*slowly*" and "*rapidly*" mobile groups. A third group, considered immobile, corresponds to molecules that move in domains whose size is below our resolution threshold: these are not represented in the graphs. For each group, generation of the mean square displacement $\langle r^2(t)\rangle$ as a function of t represents the averaged MSD of the population (Fig. 2B). This approach allowed us to analyze multiple diffusion types in each compartment without an arbitrary categorization of each individual molecule. The type of movement was then determined selecting the best fit to the mean MSD between the linear equation describing Brownian motion and the equation proposed by Kusumi et al. (1993) for confined diffusion. We obtained the characteristic size L of the area of diffusion and used this value to compare the relative degrees of confinement of each molecule.

In extrasynaptic membranes, rapidly mobile molecules all displayed similar behavior: their diffusion constant was fast (in the order of 1–2 $\mu m^2/s$) but their area of diffusion was restricted, probably by the geometry of the neurite (Fig. 2B). By contrast, we found major differences in the slowly mobile group: while AMPARs and ChTx displayed confined diffusion to domains of similar sizes ($L = 319 \pm 12$ nm for AMPARs, $L = 322 \pm 6$ nm for ChTx), DOPE displayed free diffusion (Fig. 2B).

At synapses, all molecules displayed confined movements (Fig. 2B). To test whether this behavior was due to our method of analysis, we randomly generated domains of similar sizes to Rh123 stains in the extrasynaptic membrane. Applying the same

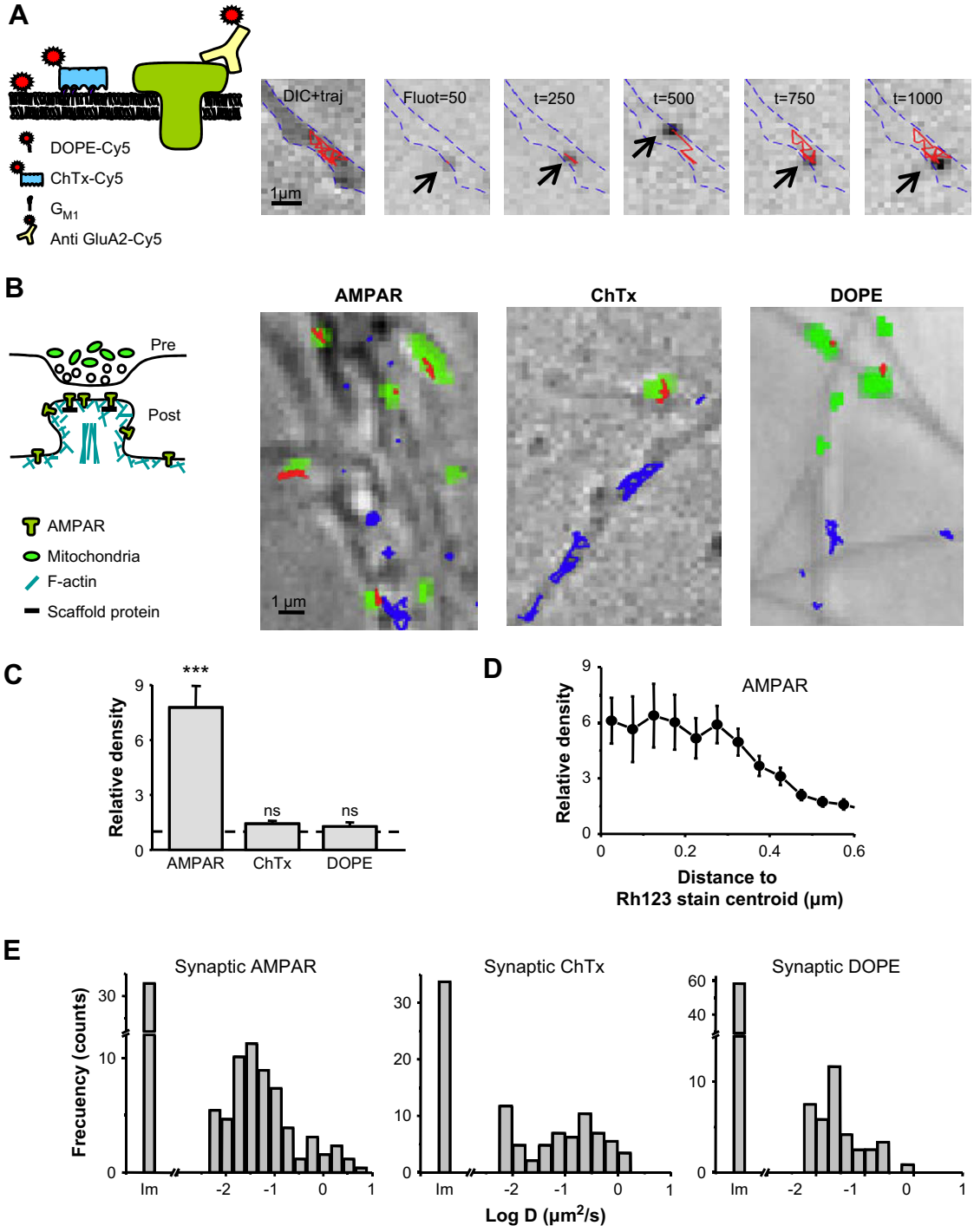

Fig. 1. Single molecule tracking of AMPARs and lipids in live hippocampal neurons in culture. (A) Left: schematic diagram of the molecules studied. DOPE was directly labeled with Cy5, G_{M1} was tracked by Cy5-coupled cholera toxin (ChTx) and GluA2-containing AMPARs were tracked with Cy5-labeled anti-GluA2. Right: DIC + traj: DIC image of a neurite overlaid with the trajectory (red) of the molecule shown in the right micrographs over 1 s. Fluo: sequence of five fluorescence images (inverted hue) taken at 200–250 ms interval. The arrows indicate the position of the molecule as detected by the tracking algorithm. The partial trajectory of the molecule up to the indicated time is overlaid in red. (B) Left: synapses were labeled by the mitochondrial marker rhodamine123 (Rh123). Right: whole field DIC images of neurites (fields of recording) showing in green the synaptic staining of Rh123. Synaptic molecules were defined as the ones co-localizing with an Rh123 stain. The trajectories of all the single molecules detected in this field over a 100 s recording period are overlaid in blue (extrasynaptic) or in red (synaptic). (C) Enrichment of AMPARs in synapses. The density of molecules detected co-localizing with the synaptic staining was compared with the density obtained in areas of equivalent size positioned randomly over neurite portions bearing no Rh123 staining (normalized to 1, indicated by the striped line) ($n = 40$ fields of recording, ns: not significant, $^{***}p < 0.001$ t test). (D) Relative number of labeled AMPARs on Rh123 stains measured as the distance between the fluorescent spot of the molecule and the centroid of the stain ($n = 2059$). (E) Frequency histograms of instantaneous diffusion coefficient D in synaptic areas for AMPAR ($n = 153$), ChTx ($n = 68$) and DOPE ($n = 57$), normalized to the total number of molecules. Molecules having D below 0.005 µm²/s were considered immobile (Im).

analysis, we found that the fraction of extrasynaptic trajectories that co-localized with these simulated synapses did not display a confined signature. Thus the confinement observed is specific to synapses.

At synapses, large differences were found in the area over which the molecules diffused depending on the type of molecule (Fig. 2C). Rapidly mobile AMPARs and ChTx were confined to domains of ±600/700 nm in diameter while rapidly mobile DOPE was confined

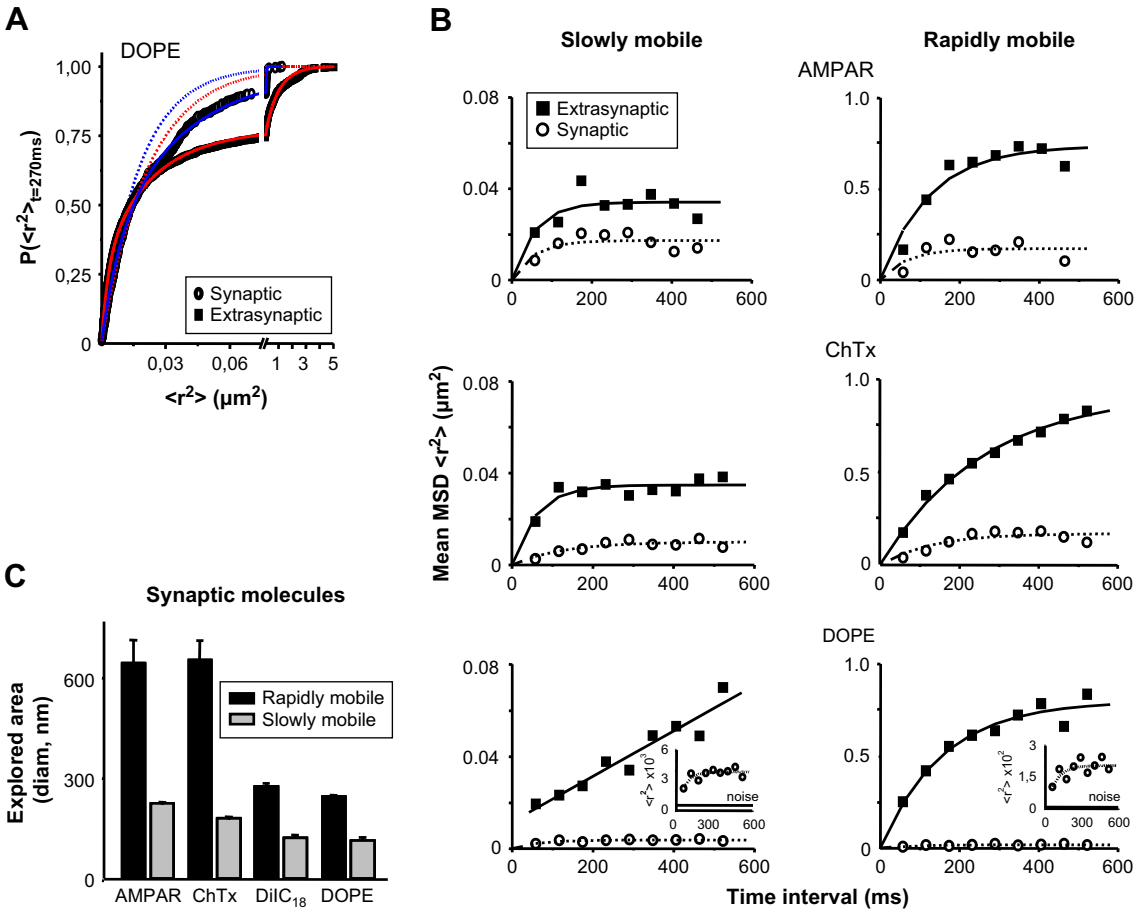

Fig. 2. Modes of diffusion in extrasynaptic and synaptic areas. (A) Cumulative probability distribution of the square displacements r^2 for DOPE at the interval of time $t = 270$ ms; for extrasynaptic (black squares and red lines) and synaptic (white circles and blue lines) trajectories of mobile molecules. The curves were fitted with a one-exponential equation (dotted lines) or a two-exponential equation (full lines) (see Section 4). The best fits obtained with the double-exponential curves indicate that there are two groups of mobile molecules with different mobility behavior. (B) Modes of diffusion of AMPAR ($n = 570$), ChTx ($n = 1321$) and DOPE ($n = 598$) in extrasynaptic (black squares) and synaptic areas (white circles), for the slowly mobile and the rapidly mobile population. Each point is the mean MSD ($\langle r^2 \rangle$) of each subgroup obtained as the coefficients of the fit over $P(\langle r^2 \rangle)$ (see Fig. 2A). Data were fitted with the equation describing confined movement $\langle r^2 \rangle = L^2/3(1 - \exp(-12Dt/L^2))$, (Kusumi et al., 1993) or with a linear fit. In all cases, the movement detected was well above the noise level (inset in the graph of DOPE). (C) In the case of confinement, the value L obtained from the equation indicated above is the diameter of the available area for diffusion. The values of L (mean ± SE) in synapses are shown for all the molecules studied, for the slowly mobile (gray bars) and the rapidly mobile group (black bars) (at least four independent experiments). (For interpretation of colour in this figure, the reader is referred to the web version of this article.)

to smaller domains (approx. 250 nm). Slowly mobile molecules were confined to even smaller domains, with decreasing sizes for AMPAR, ChTx and DOPE (Fig. 2C, Table 1).

Surprisingly, DOPE displayed the smallest area of diffusion (±110 nm, well above our detection threshold as seen in Fig. 2B insets). To confirm this result we performed similar experiments using $DiIC_{18}$, a fluorescent lipid-raft marker. In the extrasynaptic membrane, $DiIC_{18}$ revealed a lower D than DOPE (Table 1) and displayed confined diffusion (slowly mobile group: $L = 240 \pm 6$ nm, rapidly mobile group: $L = 844 \pm 29$ nm). In synapses, however, both lipids displayed a similar degree of confinement (Fig. 2C, Table 1) independently of their raft or non-raft character. Therefore at the synaptic membrane the smaller molecules were the most confined.

2.4. Glutamate increases the diffusion of molecules

Bath application of glutamate decreases the quantity of AMPARs at synapses and targets them to internalization, a protocol proposed to mimic LTD (Carroll et al., 1999; Lissin et al., 1999).

We noted the degree of reduction in AMPARs at synapses: control, 7.97 ± 1.26-fold increase over the density on the extrasynaptic membrane; glutamate 1–10 min, 6.33 ± 0.87-fold, glutamate 10–20 min, 5.51 ± 0.55-fold, $p < 0.05$ t test, while the

Table 1
Diameter L of the area explored by the different molecules in synapses (mean ± SE), calculated from $\langle r^2 \rangle = L^2/3(1 - \exp(-12Dt/L^2))$ (Kusumi et al., 1993)

	Slowly mobile group				Rapidly mobile group			
	AMPAR	ChTx	DOPE	$DiIC_{18}$	AMPAR	ChTx	DOPE	$DiIC_{18}$
Control	225 ± 3	182 ± 9	116 ± 9	123 ± 7	645 ± 74	655 ± 63	246 ± 9	277 ± 14
Glutamate applied	239 ± 15	233 ± 8***	124 ± 5		n/d	679 ± 49*	n/d	

n/d: Not determined.
*$p < 0.05$, **$p > 0.01$, ***$p < 0.001$, t test.

distribution of lipid molecules did not change (not shown). The quantity of immobile receptors in synapses was reduced over time (control: 43.14 ± 1.82%, glutamate 1–10 min: 33.20 ± 1.74%, $p < 0.01$ *t* test). There was also a decrease in the quantity of mobile molecules observed only after 10–20 min.

The reduction in the enrichment of AMPARs at synapses was correlated with an increase in mobility revealed by both *D* (35% increase, $p < 0.05$ MW) and the reduction of confinement (Fig. 3A, Table 1). Lipids also displayed a reduction in confinement in the presence of glutamate (Fig. 3A, Table 1). Similar results were obtained between 1 and 10 min and between 10 and 20 min of glutamate application for all the molecules studied.

3. Discussion

We compared the lateral diffusion of AMPARs and different lipids inside and outside synapses of mature hippocampal neurons in culture. The observed complexity of AMPAR diffusion behavior is a consequence of several effects related to their stabilization by interactions with scaffolding proteins as well as to transient and non-specific interactions with obstacles to diffusion. The analysis of the diffusion of lipids allowed us to compare the mobility of AMPARs with that of molecules not enriched at synapses and thus not stabilized by the scaffold.

Despite differences in terms of size and insertion in the membrane, receptors and lipids exhibited a wide but similar range of diffusion coefficient *D* which was lower inside synapses than at the extrasynaptic membrane. To study the diffusion behavior of molecules with such a wide distribution of *D*, we used an analytical method which revealed groups of molecules with different mobilities. We identified two main populations of mobile molecules for AMPAR, ChTx and DOPE, both in extrasynaptic and synaptic areas. Interestingly, they displayed different behavior depending on the compartment (synaptic or extrasynaptic membrane) and the molecule type. At the extrasynaptic membrane, the lateral diffusion of the rapidly mobile group was restricted only by the geometry of the neurite for the three molecules studied. Slowly mobile molecules however were free in the case of DOPE but confined in the cases of AMPAR and ChTx. In contrast and within the time-frame of our observations, molecules detected in synapses showed more stringent limitations to diffusion in all cases.

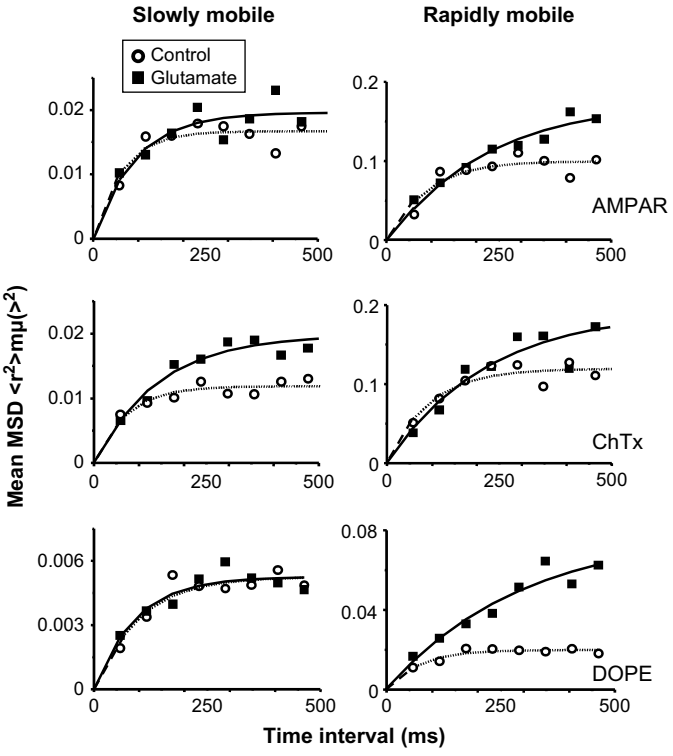

Fig. 3. Modes of diffusion after glutamate application. (A) Modes of diffusion for synaptic AMPAR (control $n = 287$; glutamate $n = 212$), ChTx (control $n = 92$; glutamate $n = 169$) and DOPE (control, $n = 186$; glutamate, $n = 279$) in control cells (white circles) or in cells incubated within 1 and 10 min with glutamate (black squares). The mean MSD ($\langle r^2 \rangle$) and fits were calculated as in Fig. 2B.

Not only AMPARs but also lipids displayed confined diffusion in mature synapses. They diffused over areas of various sizes from 100 to 700 nm in diameter, in the range of the PSD size (Fiala and Harris, 2001). We could not ascertain which trajectory represented a lipid at the presynaptic or the postsynaptic membrane. However, the large difference in diffusion behavior found between the synaptic and the extrasynaptic molecules suggests that their mobility was reduced in both synaptic membranes, although we could not determine whether the two diffusion areas were different.

An unexpected result was that the smaller molecules, DOPE and $DiIC_{18}$, diffused over smaller areas than ChTx or AMPARs. Indeed, ChTx diffused similarly to the receptor instead of diffusing like $DiIC_{18}$, another lipid-raft marker. Rapidly mobile lipids (DOPE and $DiIC_{18}$) showed similar confinement to the slowly mobile receptors or ChTx (diffused over approximately 200 nm) whereas slowly mobile lipids move over even smaller areas (around 100 nm).

DOPE and $DiIC_{18}$ displayed different diffusion behavior in the extrasynaptic membrane suggesting a heterogeneous lipid composition and that the 'raft-like' characteristics of $DiIC_{18}$ dictate its diffusion properties outside synapses. Strikingly, synaptic DOPE and $DiIC_{18}$ displayed similar confinement properties. This hints that restrictions to diffusion in synapses do not primarily depend on their lipid composition but rather on spatial steric effects. This is supported by the similar confinement properties of mobile ChTx and AMPARs, which thus probably encounter the same restrictions to diffusion. Altogether, our observations support the idea that the synaptic membrane constitutes a crowded environment with tiny areas between immobilized proteins that are accessible only to the smaller molecules, such as DOPE and $DiIC_{18}$. This is similar in mode of action to a size exclusion column.

We measured a mean instantaneous diffusion rate for DOPE comparable to those of receptors although a much faster diffusion should be expected for lipids. Kusumi et al. (1993) studied the diffusion behavior of DOPE in several cell types. Using very fast acquisition frequency, they found that it undergoes 'hop diffusion' in the plasma membrane, diffusing very rapidly but in a confined fashion, and hopping periodically between adjacent compartments (Fujiwara et al., 2002; Suzuki et al., 2005). It is likely that our experiments could not determine *D* inside these compartments nor the hopping behavior of DOPE. We thus probably measured the apparent diffusion of DOPE slowed down by the hopping behavior (Ritchie et al., 2005). This would explain the free but slow diffusion observed for the slowly mobile group in the extrasynaptic membrane.

While all molecules studied here displayed confinement, only receptors were enriched at synapses. Barriers to diffusion cannot by themselves explain the local enrichment of receptors. To concentrate them at the PSD, stable interactions with scaffolding elements are needed. These may originate from interactions with PDZ-domain-containing scaffold proteins (Bats et al., 2007) and cytoskeleton elements such as F-actin (Schulz et al., 2004) that could represent scaffolding sites itself, or stabilize. Interestingly, the bath application of glutamate increased the mobility of all molecules and lowered their confinement. Glutamate decreases the quantity of AMPARs at synapses and targets them to internalization, a protocol proposed to mimic LTD (Carroll et al., 1999; Lissin et al., 1999). The

glutamate-induced dissociation of AMPARs from their anchor on the postsynaptic membrane has been suggested to involve actin depolymerization (Zhou et al., 2001), allowing the released AMPARs to segregate from the NMDARs and diffuse to a presumably perisynaptic site, where they become available to an endocytotic machinery and are selectively internalized. The increased mobility we observed is fully consistent with this model and suggests further that glutamate treatment loosens the diffusion barriers to allow AMPARs to leave the PSD rapidly.

4. Experimental procedures

4.1. Microscopy and single-molecule/single particle detection

For SMT experiments, an inverted microscope (Olympus IX70; Olympus, France) with a 100× oil-immersion objective (NA = 1.4) was used. For Cy5 detection samples were illuminated for 15 ms at 633 nm by a He–Ne laser (JDS Uniphase, USA) at 18 Hz. A defocusing lens permitted illumination of 20×20 mm^2 with an intensity of 7 ± 1 kW/cm^2. A filter set (DCLP650, HQ575/50; Chroma Technology, USA) permitted the detection of individual fluorophores by a back-illuminated CCD camera (Micromax Princeton Instruments, USA). The total detection efficiency was approximately 5%. In the case of quantum dots (QDs), cells were imaged with a 60× objective (NA = 1.45, Olympus) using a xenon lamp and appropriate excitation filters (HQ500/20×, Chroma Technology, USA; 560RDF55, Omega Optical, USA) and emission filters (HQ560/80M, Croma; 655WB20, Omega). Signals were detected using a CCD camera (Cascade 512BFT; Roper Scientific, USA). Rh123 was imaged using a 532 nm frequency doubled YAG laser (Coherent, France) at an illuminating intensity of 3 kW/cm^2 using another filter set (DCLP498, Chroma; A515, Omega).

4.2. Labeling of ChTx, GluA2 antibody or DOPE for single molecule tracking

Cy5 fluorophore was coupled to cholera toxin (ChTx; Sigma Aldrich, France) at a mean ratio of 1:7 following the manufacturer's instructions (Amersham Biosciences, UK) to yield 85–90% of the ChTx with only one fluorophore. Similarly, Cy5 was coupled to GluA2 antibody (BD Pharmingen, Belgium) at 1:1.5 ratio. For DOPE labeling, Cy5 diluted in methanol was used mixed with DOPE (from a chloroform solution; Avanti Polar Lipids, USA) at 1:1 ratio. After 60 min of incubation at room temperature, the sample was passed through a C_{18} column (Waters, France). A 1:1 mixture of methanol/water was used to wash out the free dye and DOPE-Cy5 was eluted in methanol.

4.3. Cell culture and treatments

Hippocampal neurons from 18-day-old rat embryos were cultured on glass coverslips following the Banker technique. For synapse staining, coverslips were first incubated at 37 °C for 5 min with 2 mM rhodamine 123 (Rh123; Molecular Probes, The Netherlands) and then incubated for 10 min at room temperature with the labeled ligand. In the case of DOPE or $DiIC_{18}$ (Interchim, France), cells were incubated for 15 min at room temperature with the labeled lipid. The coverslips were then extensively rinsed and mounted in a custom chamber with culture medium at 37 °C. In the case of QDs, 655 Goat F(ab')2 anti-Rabbit IgG conjugates were used (Quantum Dot Corp., Ozyme, France), previously incubated with casein for 15 min to block unspecific binding. Cells were incubated for 10 min at room temperature with anti-GluA2 antibody and then with QDs (final dilution 1:10,000) and extensively rinsed with culture medium.

Glutamate (100 μM) was applied either after recording movies in the control conditions, or immediately before the beginning of the experiment. On a few occasions, we observed rapid movements of Rh123 stains that we attributed to vesicle trafficking and these recordings were discarded.

4.4. Trajectory construction and analysis

All labels were used at low concentration to ascertain discrimination of fluorescent spots arising from single fluorophores. Only those that had the hallmarks of individual fluorescent molecules (i.e., one-step photobleaching and characteristic intensity) were retained for analysis. Images were obtained at a frequency of 18 Hz for the tracking of Cy5 fluorophores. The spatial distribution of the signals was fitted to a two-dimensional Gaussian surface with a full-width at half-maximum of 360 ± 40 nm, given by the point-spread function of our set-up. The two-dimensional trajectories of molecules in the plane of focus were constructed from the image series by correlation analysis using a Vogel algorithm (Schütz et al., 1997). Only trajectories containing at least four points were retained. Measurements done on individual fluorescent molecules dried on glass showed that pointing accuracy is $45 + 5$ nm.

The instantaneous diffusion coefficient D for each trajectory was calculated from linear fits of the first four points (corresponding to approx. 200 ms) of the mean square displacement (MSD) plot using: $\mathrm{MSD}(t) = 4Dt$ (Kusumi et al., 1993; Serge et al., 2002). SMT trajectories were typically 0.4–0.5 s long while QD trajectories were constructed from up to 500 consecutive frames (25 s long).

To investigate the diffusion behavior, trajectories were analyzed following a method described by Schütz et al. (1997). In brief, the probability that Brownian particles starting to diffuse from the origin will be found within a circle of radius r at time t is given by

$$P\left(r^2, t\right) = 1 - \exp\left(-t/r^2\right) \tag{1}$$

If there are more than one group of particles with different mobility (i.e., three groups) Eq. (1) becomes

$$P\left(r^2, t\right) = p_1\left(1 - \exp\left(-t/r_1^2\right)\right) + p_2\left(1 - \exp\left(-t/r_2^2\right)\right) + p_3\left(1 - \exp\left(-t/r_3^2\right)\right) \tag{2}$$

where p_i are the relative amounts of each sub-population.

A least-square fit to Eq. (2) leads to a robust estimation of the mean MSD $\langle r_i^2 \rangle$ of each population even when the mobility is not purely random. By plotting r_i^2 versus t, the diffusion behavior of the respective sub-populations of molecules is revealed. In the case of confined diffusion, this plot was fitted to

$$r^2 = L^2/3\left(1 - \exp\left(-12Dt/L^2\right)\right) \tag{3}$$

where L is the diameter of the confinement area (Kusumi et al., 1993).

Only probability distributions with more than 150 data points were fitted by Eq. (2). For each analysis, the calculation was carried out on at least four independent experiments (40 different fields of recording).

The robustness of the analysis was tested performing Monte Carlo simulations of random walking trajectories. We constructed trajectories for each generated molecule similar to those obtained experimentally (D and length) but with the successive positions chosen at random. The trajectories analyzed as above yielded linear dependencies of $\langle r^2 \rangle$ with time for all the mobility groups. Thus, the anomalous diffusion detected by this method does not arise from random fluctuations of Brownian motion.

4.5. Synaptic localization and simulation

We used a mitochondrial marker (Rh123) to stain mitochondria which accumulate in presynaptic terminals (Fig. 1A and 2A). Concentration and incubation time were adjusted to stain only the presynaptic terminal, as confirmed by co-staining with synaptotagmin (Groc et al., 2004; Tardin et al., 2003). The images of synaptic staining were filtered using a wavelets algorithm (Groc et al., 2007) and binarized. Trajectories were then sorted automatically into synaptic and extrasynaptic by their co-localization with Rh123 stains. In the case of molecules that change localization during the recording, their trajectories were dissected to analyze each part separately. In order to estimate the effect of trajectory sorting and dissection on our analysis, we generated simulated synaptic areas using the size distribution of the Rh123 stains. Extrasynaptic trajectories were randomly assigned to these compartments and dissected if necessary. Results from real synaptic trajectories were then compared with these simulated data.

Acknowledgements

We thank C. Breillat and D. Bouchet for valuable help in carrying out molecular biology and cell culture work. This work was supported by grants from the Centre National de la Recherche Scientifique, the Conseil Régional d'Aquitaine, the Ministère de la Recherche, the Fondation pour la Recherche Médicale, the Association Française contre les Myopathies and the European Community Grant QLG3-CT-2001-02089.

References

Bats, C., Groc, L., Choquet, D., 2007. The interaction between Stargazin and PSD-95 regulates AMPA receptor surface trafficking. Neuron 53, 719–734.
Blanpied, T.A., Scott, D.B., Ehlers, M.D., 2002. Dynamics and regulation of clathrin coats at specialized endocytic zones of dendrites and spines. Neuron 36, 435–449.
Borgdorff, A.J., Choquet, D., 2002. Regulation of AMPA receptor lateral movements. Nature 417, 649–653.
Bredt, D.S., Nicoll, R.A., 2003. AMPA receptor trafficking at excitatory synapses. Neuron 40, 361–379.
Carroll, R.C., Lissin, D.V., von Zastrow, M., Nicoll, R.A., Malenka, R.C., 1999. Rapid redistribution of glutamate receptors contributes to long-term depression in hippocampal cultures. Nat. Neurosci. 2, 454–460.
Chen, L., Chetkovich, D.M., Petralia, R.S., Sweeney, N.T., Kawasaki, Y., Wenthold, R.J., Bredt, D.S., Nicoll, R.A., 2000. Stargazing regulates synaptic targeting of AMPA receptors by two distinct mechanisms. Nature 408, 936–943.
Choquet, D., Triller, A., 2003. The role of receptor diffusion in the organization of the postsynaptic membrane. Nat. Rev. Neurosci. 4, 251–265.
Dahan, M., Levi, S., Luccardini, C., Rostaing, P., Riveau, B., Triller, A., 2003. Diffusion dynamics of glycine receptors revealed by single-quantum dot tracking. Science 302, 442–445.
Dietrich, C., Yang, B., Fujiwara, T., Kusumi, A., Jacobson, K., 2002. Relationship of lipid rafts to transient confinement zones detected by single particle tracking. Biophys. J. 82, 274–284.
Dong, H., O'Brien, R.J., Fung, E.T., Lanahan, A.A., Worley, P.F., Huganir, R.L., 1997. GRIP: a synaptic PDZ domain-containing protein that interacts with AMPA receptors. Nature 386, 279–284.
Fiala, J.C., Harris, K.M., 2001. Extending unbiased stereology of brain ultrastructure to three-dimensional volumes. J. Am. Med. Inform. Assoc. 8, 1–16.
Fujiwara, T., Ritchie, K., Murakoshi, H., Jacobson, K., Kusumi, A., 2002. Phospholipids undergo hop diffusion in compartmentalized cell membrane. J. Cell Biol. 157, 1071–1081.
Fukata, Y., Tzingounis, A.V., Trinidad, J.C., Fukata, M., Burlingame, A.L., Nicoll, R.A., Bredt, D.S., 2005. Molecular constituents of neuronal AMPA receptors. J. Cell Biol. 169, 399–404.
Groc, L., Heine, M., Cognet, L., Brickley, K., Stephenson, F.A., Lounis, B., Choquet, D., 2004. Differential activity-dependent regulation of the lateral mobilities of AMPA and NMDA receptors. Nat. Neurosci. 7, 695–696.
Groc, L., Lafourcade, M., Heine, M., Renner, M., Racine, V., Sibarita, J.B., Lounis, B., Choquet, D., Cognet, L., 2007. Surface trafficking of neurotransmitter receptor: comparison between single-molecule/quantum dot strategies. J. Neurosci. 27, 12433–12437.
Heine, M., Groc, L., Frischknecht, R., Beique, J.C., Lounis, B., Rumbaugh, G., Huganir, R.L., Cognet, L., Choquet, D., 2008. Surface mobility of postsynaptic AMPARs tunes synaptic transmission. Science 320, 201–205.
Kusumi, A., Sako, Y., Yamamoto, M., 1993. Confined lateral diffusion of membrane receptors as studied by single particle tracking (nanovid microscopy). Effects of calcium-induced differentiation in cultured epithelial cells. Biophys. J. 65, 2021–2040.
Lisman, J.E., Zhabotinsky, A.M., 2001. A model of synaptic memory: a CaMKII/PP1 switch that potentiates transmission by organizing an AMPA receptor anchoring assembly. Neuron 31, 191–201.
Lissin, D.V., Carroll, R.C., Nicoll, R.A., Malenka, R.C., von Zastrow, M., 1999. Rapid, activation-induced redistribution of ionotropic glutamate receptors in cultured hippocampal neurons. J. Neurosci. 19, 1263–1272.
Malinow, R., Malenka, R.C., 2002. AMPA receptor trafficking and synaptic plasticity. Ann. Rev. Neurosci. 25, 103–126.
Meier, J., Vannier, C., Sergé, A., Triller, A., Choquet, D., 2001. Fast and reversible trapping of surface glycine receptors by gephyrin. Nat. Neurosci. 4, 253–260.
Racz, B., Blanpied, T.A., Ehlers, M.D., Weinberg, R.J., 2004. Lateral organization of endocytic machinery in dendritic spines. Nat. Neurosci. 7, 917–918.
Ritchie, K., Shan, X.Y., Kondo, J., Iwasawa, K., Fujiwara, T., Kusumi, A., 2005. Detection of non-Brownian diffusion in the cell membrane in single molecule tracking. Biophys. J. 88, 2266–2277.
Samsonov, A.V., Mihalyov, I., Cohen, F.S., 2001. Characterization of cholesterol-sphingomyelin domains and their dynamics in bilayer membranes. Biophys. J. 81, 1486–1500.
Saxton, M.J., Jacobson, K., 1997. Single-particle tracking: applications to membrane dynamics. Ann. Rev. Biophys. Biomol. Struct. 26, 373–399.
Scannevin, R.H., Huganir, R.L., 2000. Postsynaptic organization and regulation of excitatory synapses. Nat. Rev. Neurosci. 1, 133–141.
Schnell, E., Sizemore, M., Karimzadegan, S., Chen, L., Bredt, D.S., Nicoll, R.A., 2002. Direct interactions between PSD-95 and stargazin control synaptic AMPA receptor number. Proc. Nat. Acad. Sci. U.S.A. 99, 13902–13907.
Schütz, G.J., Schindler, H., Schmidt, T., 1997. Single-molecule microscopy on model membranes reveals anomalous diffusion. Biophys. J. 73 (2), 1073–1080.
Schulz, T.W., Nakagawa, T., Licznerski, P., Pawlak, V., Kolleker, A., Rozov, A., Kim, J., Dittgen, T., Kohr, G., Sheng, M., Seeburg, P.H., Osten, P., 2004. Actin/alpha-actinin-dependent transport of AMPA receptors in dendritic spines: role of the PDZ-LIM protein RIL. J. Neurosci. 24, 8584–8594.
Serge, A., Fourgeaud, L., Hemar, A., Choquet, D., 2002. Receptor activation and homer differentially control the lateral mobility of metabotropic glutamate receptor 5 in the neuronal membrane. J. Neurosci. 22, 3910–3920.
Sheng, M., Kim, M.J., 2002. Postsynaptic signaling and plasticity mechanisms. Science 298, 776–780.
Shepherd, J.D., Huganir, R.L., 2007. The cell biology of synaptic plasticity: AMPA receptor trafficking. Ann. Rev. Cell Dev. Biol. 23, 613–643.
Spink, C.H., Yeager, M.D., Feigenson, G.W., 1990. Partitioning behavior of indocarbocyanine probes between coexisting gel and fluid phases in model membranes. Biochim. Biophys. Acta 1023, 25–33.
Suzuki, K., Ritchie, K., Kajikawa, E., Fujiwara, T., Kusumi, A., 2005. Rapid hop diffusion of a G-protein-coupled receptor in the plasma membrane as revealed by single-molecule techniques. Biophys. J. 88, 3659–3680.
Tardin, C., Cognet, L., Bats, C., Lounis, B., Choquet, D., 2003. Direct imaging of lateral movements of AMPA receptors inside synapses. EMBO J. 22, 4656–4665.
Terashima, A., Cotton, L., Dev, K.K., Meyer, G., Zaman, S., Duprat, F., Henley, J.M., Collingridge, G.L., Isaac, J.T., 2004. Regulation of synaptic strength and AMPA receptor subunit composition by PICK1. J. Neurosci. 24, 5381–5390.
Triller, A., Choquet, D., 2005. Surface trafficking of receptors between synaptic and extrasynaptic membranes: and yet they do move!. Trends Neurosci. 28, 133–139.
Zhou, Q., Xiao, M., Nicoll, R.A., 2001. Contribution of cytoskeleton to the internalization of AMPA receptors. Proc. Nat. Acad. Sci. U.S.A. 98, 1261–1266.